ELSEVIER

Physica D 98 (1996) 53–66

PHYSICA D

From quasi-2D to 3D Turing patterns in ramped systems

E. Dulos *, P. Davies, B. Rudovics, P. De Kepper

Centre de Recherche Paul Pascal, CNRS, Université Bordeaux I, Avenue Schweitzer, 33600 Pessac, France

Received 18 December 1995; revised 8 March 1996; accepted 8 March 1996
Communicated by F.H. Busse

Abstract

We elaborate on the transition from quasi-two-dimensional to three-dimensional Turing patterns in a chemical reaction–diffusion system confined in gradients of chemicals between two feed boundaries. This transition is observed in open spatial reactors specially designed to make possible the unfolding of a pattern sequence in one direction of the plane of observation. In this direction, the confinement of the structure is progressively relaxed. Complementary observations from two reactor geometries allow the dimensionality of the structure to be elucidated: quasi-two-dimensional and three-dimensional patterns, respectively, correspond to patterns developing in monolayers and in bilayers. Beyond the now classical hexagonal and stripe patterns, various new stable planforms are shown to result from the coupling of these two classical pattern modes which develop in two adjacent layers, with well-defined phase relations between the two pattern modes.

PACS: 05.70.Ln, 47.54.+r; 82.20.Mj; 80.
Keywords: Turing patterns; Reaction–diffusion; Pattern dimensionality; Confined systems; CIMA reaction

1. Introduction

Turing patterns belong to the class of self-organization phenomena that result from a spontaneous symmetry breaking instability in non-linear dynamical systems maintained at a controlled distance from thermodynamic equilibrium. These are stationary concentration patterns of solvated species that result from the sole interplay of molecular diffusion and chemical reaction. Such chemical reactions must involve antagonistic activatory and inhibitory kinetic processes. Turing patterns call for differences in the diffusion coefficients of species, in particular, a species controlling the inhibitory process must diffuse faster than species in control of the activatory process. The patterns are characterized by an intrinsic wavelength, that is wavelength is independent of any geometric dimension of the system. Due to seemingly contradictory requirements for their formation, the first unambiguous experimental observation of Turing patterns [1] occurred nearly 40 years after their theoretical prediction by Turing in 1952 [2]. Besides their fundamental interest in physics [3], their possible implication in certain stages of morphogenesis made them popular among a community of biologists and biomathematicians [4–6].

Most of the theoretical works on pattern formation assume, for mathematical simplicity, that the system be uniformly constrained over space. Under these conditions, it has been analytically determined and confirmed by numerical simulations that only a small number of planforms can spontaneously develop. In

* Corresponding author.

PII S0167-2789(96)00072-3

two-dimensional systems, these planforms consist of hexagonal arrays of dots and parallel stripe patterns [7–9]. In three-dimensional systems, lamella, hexagonal prisms and body centered cubic arrays [10] are such selected patterns.

It is worth noting that in real chemical systems, it is impossible to fulfil the uniform constraint conditions. As we shall see in more detail further on, the experimentally observed Turing patterns develop in systems that naturally involve parameter gradients. These gradients confine the pattern in a more or less narrow region of space where appropriate chemical conditions are met for the Turing instability to develop.

Nonetheless, the effect of parameter gradients in a chemical one-dimensional system was considered form a theoretical point of view during 1970's [11]. It was also theoretically examined in two- or three-dimensional systems, in the framework of patterning models for biological systems [12,13]. In this context, Boissonade [14] provided in 1988 a numerical analysis of a Turing bifurcation in a two-dimensional rectangular system fed only by diffusion from two opposite boundaries, a configuration which naturally leads to gradients of feeding species. These calculations show that at onset, the Turing instability develops a dot pattern orthogonally to the parameter gradients. Our initial experimental observation of sustained Turing patterns followed this more practical approach [1].

Using the CIMA reaction, we have observed patterns developing in successive rows of spots [1,15,16], in perfect agreement with Boissonade's theoretical results [14,16]. Soon after, with the same reaction and a reactor more extended in the third direction, Ouyang and Swinney produced spot and stripe patterns [17,18] analogue to those predicted in extended two-dimensional systems; these patterns tessellate planes that extend in the third direction of the reactor. Some of our experiments indicated that pattern can be three-dimensional [19]. Ouyang et al. rather produced apparently two-dimensional patterns [17,18,20]; then, they also considered the development of three-dimensional patterns. Further experimental observations show that different patterns can develop at different distances to the feed boundaries [21] and that the dimensionality of patterns may depend on some geometric size of the reactor [22]. More recently, we have published a preliminary observation of three-dimensional patterns consisting either of two contiguous planes tessellated with stationary patterns or of one plane of stationary patterns and one with travelling waves [23,24].

Here, we report on experiments performed in reactors designed to elucidate how two-dimensional patterns evolve to three-dimensional patterns as the confinement in the third direction is gradually relaxed. We also examine the transition between different types of two-dimensional patterns under a slow parameter ramp. We emphasize that there are no genuine two-dimensional experimental patterns but rather patterns developing in monolayers and we discuss the experimental patterns in monolayers in connection with actually two-dimensional patterns produced by simulations. The experimental conditions (reactors and reaction) used for the reported experiments are indicated in Section 2. We describe in Section 3 the patterns observed first in the asymptotic state of the system, then in a transient situation. Finally these experimental results are discussed in Section 4, in the light of results of theoretical studies and simulations of such systems, and taking into account the dimensionality of the patterns.

2. Experimental conditions

2.1. Reactor

The core of the reactor is a piece of soft hydrogel with two opposite faces in contact with solutions of reagents kept in two reservoirs I and II (see Fig. 1(a)). Starting from these faces, reagents diffuse into the gel where they meet and react. The other sides of the piece of gel correspond to impermeable boundaries. The gel prevents the chemical reacting medium from any convective fluid motion so that the only active processes inside the gel are the reaction and the molecular diffusion of species. Solutions in reservoirs I and II are permanently renewed by pumps and continuously stirred, ensuring constant and uniform boundary conditions. Reagents are distributed in

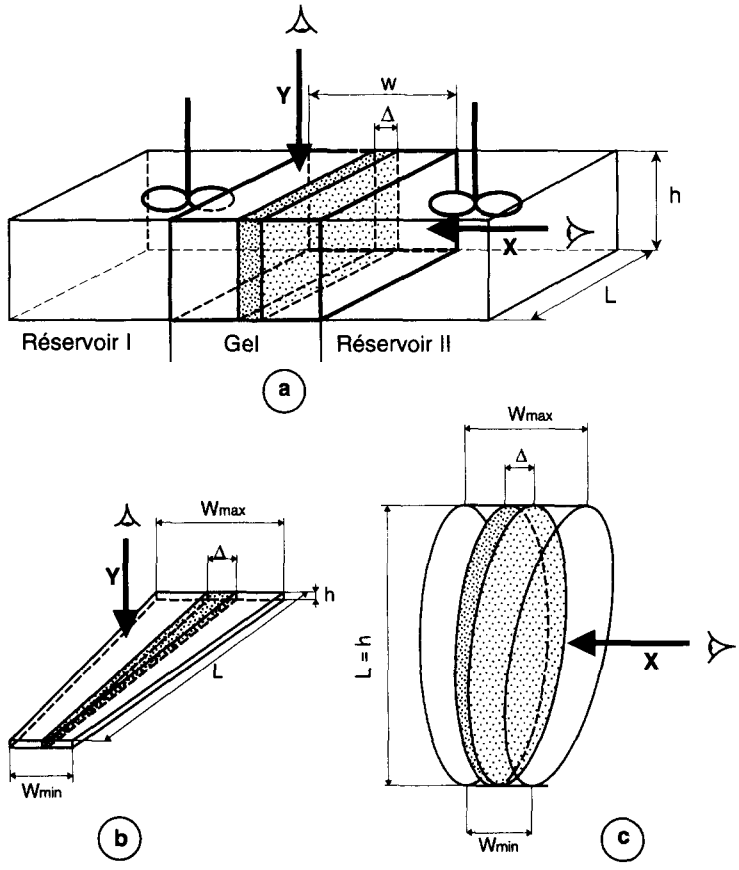

Fig. 1. Sketches of the open spatial reactors. (a) The basic principle: the piece of gel ($L \times h \times w$) is in contact with the contents of stirred reservoirs I and II; Δ is the width of the pattern-forming region. Observations are made from above (arrow y) in the thin strip reactor (with dimensions $h \leq w < L$), and perpendicularly to the feed surfaces in the disc reactor (diameter $L = h$). (b) and (c) The bevelled thin strip and disc reactors. In the thin strip $h = 0.2$ mm; in both reactors: $W_{max} = 3.5$ mm, $W_{min} = 1.75$ mm, $L = 25$ mm; Arrows y and x indicate the observation directions.

reservoirs I and II in such a way that neither of the solutions is separately reactive and, due to the differences in their compositions, strong concentration gradients of chemicals naturally settle in the gel perpendicularly to the feed surfaces, leading to iso-concentration planes parallel to these surfaces. Generally, the appropriate conditions for the development of a reaction–diffusion instability are only met in a restricted region of width Δ between the two feed surfaces: Δ depends on such parameters as the concentrations of feed species and, of course, on the distance w between the feed surfaces. Depending on how the wavelength λ of the pattern compares with the dimensions Δ, L and h of the pattern-forming region (Fig. 1(a)), one-, two- or three-dimensional spatial patterns can develop.

Two different geometries of reactors – the thin strip reactor and the disc reactor – have been derived from the general scheme in Fig. 1(a) as follows.

2.1.1. *Thin strip reactor*

The thin strip reactor is made of a thin narrow rectangular piece of gel ($L \gg w > h$; typically $h < 1$ mm). The gel strip is fed by the two long edges ($L \times h$). Observations made as above (see arrow y in Fig. 1(a)) provide a direct view of the area that extends between the feed surfaces. In particular, the location and the width Δ of the pattern-forming region

can immediately be seen. Pattern develops in rows of spots or in stripes parallel to the feed boundaries, that is orthogonal to the initial ramps of chemicals. The initial observations of Turing patterns were performed in a thin strip reactor [1,15,16]. If the gel strip is thin enough (h of the order of the wavelength λ of the structure), it approximates a two-dimensional rectangular system. Then one-dimensional or two-dimensional patterns can be obtained, depending on whether they develop on one or more rows.

2.1.2. Disc reactor

The disc reactor is made of a flat disc of gel with a thickness w. In this geometry, the faces $L \times h$ in Fig. 1(a) are circles with a diameter $L = h$. The disc is fed by these two circular faces. Observations made perpendicularly to the feed surfaces (arrow x in Fig. 1(a)) give a view of planes parallel to these faces, that is in a direction perpendicular to that used in the thin strip reactor. The disc reactor was first used by Ouyang and Swinney [17,18]. With this geometry of reactor, patterns made of arrays of spots or of stripes readily spread over the whole plane of observation. An obvious advantage of this reactor geometry is to allow for observation of patterns extended over large planar areas of uniform parameter values; but it obscures the pattern development in the third direction (that of the ramps of chemicals).

Summarizing, pattern in the thin strip reactor usually appears as rows of spots while it extends over planes in the disc reactor. Further these rows and planes are parallel to the feed boundaries in both reactor geometries.

2.1.3. Bevelled gel reactors

The reactors in Section 2.1 were slightly modified for the experiments reported here. The feed surfaces are no longer parallel but make an angle. Both bevelled thin strip and disc reactors (Figs. 1(b) and (c)) were used. In such geometries, w, the distance between the feed surfaces changes continuously from 1.75 to 3.5 mm over a length (or diameter) L of 25 mm. Thus, the feed surfaces make an angle of 4°.

The slant between the feed surfaces introduces a slow continuous change in control parameters along the plane of observation. Indeed, the gradient in w produces a gradual change in the concentration ramps across the gel, which results in a gradual change in Δ, the width of the patternforming region. As a consequence, the number of rows (or planes) of patterns gradually changes from one end to the other of the bevelled piece of gel. In addition, since the chemical processes within the gel are non-linear, the chemical composition along one row (or plane) will also gradually change. In such conditions, we can expect different types of patterns to develop in the direction of the slope.

Images were acquired with a black and white video CCD camera fitted with macrolens and attached to a personal computer. Subsequently, a picture processor was used to enhance the grey level contrasts.

2.2. Gel

Experiments were performed in a polyacrylamide gel loaded with thiodène [1]. Thiodène is an iodine colour indicator from Prolabo, containing 7% soluble starch [25], the excipient is washed out of the gel prior to use. The pieces of gel were made with a solution of the following composition per 100 ml: 2 g of acrylamide, 0.46 g of N, N'-methylenebisacrylamide, both from Aldrich and 3 g of thiodène. Polymerization occurs in about 10 mm at 0°C.

2.3. Reaction

Experiments were conducted with the chlorite–iodine–malonic acid oscillating reaction [26] currently referred as the "CIMA" reaction. Based on a skeleton kinetic mechanism of the reaction, it was proposed [27] that iodide (I^-) and chlorite (ClO_2^-) play, respectively, the roles of the activator and of the inhibitor species. It was also proposed [27–29] that starch, a macromolecule immobilized in the gel network (or any immobilie functional site of the gel), that makes a reservible complex with the activator, plays a key role in the formation of Turing patterns. This assumption was experimentally corroborated [30].

The reagents were distributed as follows in the reservoirs: Iodide and malonic acid in sulphuric acid solution were fed on one side. Iodate and chlorite in basic solution were fed on the other side. Note that on the chlorite side, the reservoir was fed with iodate instead of iodide. Indeed, when fed on this side, iodide is rapidly oxidized to iodate near the corresponding feed surface of the gel.

Since the oxidizers, chlorite and iodate, are only on one side, the oxidation capacity of the chemical medium inside the gel decreases from that side to the other. Consequently, near the chlorite side, the iodine species are oxidized and the gel remains colourless. Near the malonic acid side, iodine species are present mostly under their reduced forms I^- and I_2 which produce a dark blue complex with starch enclosed in the gel. Thus, along this side, the gel becomes dark.

The residence time was identical in both reservoirs and had the same value for both types of reactors. All feed parameters and bath temperature (4°C) were identical in reactors of both types in order to enable us to compare observations.

3. Experimental results

3.1. Global description

Figs. 2 and 3 give an example of the unfolding of patterns observed in our two types of bevelled reactors for a same set of feed concentrations. The figures provide a global view of the bevelled gel strip and disc after 36 h.

As already mentioned, the directions of observations for the two reactor geometries are orthogonal. The symmetry breaking pattern in the thin strip reactor appears as rows of spots parallel to the feed edges of the strip. In the disc reactor, a much wider variety of patterns tesselating the plane is observed.

Due to the small wavelength of the patterns (about 0.13 mm) and the pixel resolution of the CCD camera, macrolens were used to obtain pictures of patterns with enough resolution. Consequently, only a small part of the reactor is viewed at one time; the images of the whole bevelled pieces of gel can be reconstructed by placing side by side several pictures such as those presented in Figs. 2 and 3. Note that the magnification of Fig. 2 is greater than that of Fig. 3. In all the cases, larger magnifications of selected areas are provided when necessary. Note also that the focal depth of the optical set-up used in the reported experiments is of the order of 1 mm.

3.1.1. In bevelled thin strip

The experiment presented in Fig. 2 was performed with a gel strip 0.2 mm thick. The width of the strip increases from Fig. 2(a) to Fig. 2(e) and from left to right in each figure. The figures only show the side of the strip that bears patterns. Each figure exhibits from bottom to top: (i) a first dark band that develops next to the malonic acid fed boundary located along the bottom of the pictures, followed by (ii) a clear band parallel to the preceding dark one, and (iii) a second dark band parallel to the other bands, inside which a pattern of clear dots develops; the width of this band increases with the width of the strip; beyond this, (iv) a clear zone extends over the rest of the strip.

Let us now focus on the second dark band. Typically, as the width of the gel strip increases, a spot pattern emerges in that region; the spots organize in one, then two rows parallel to the feed boundaries:

- In the narrowest part of the strip (Fig. 2(a)), no spot pattern is observed: in this region of the gel, no symmetry breaking pattern develops.
- In the following part (Fig. 2(b)), the clear spot pattern breaking the boundary symmetry emerges and develops over one row. Note that the pattern becomes fuzzy at the right end of this figure.
- In the widest parts of the strip (Fig. 2(d) and (e)), the width of the region of symmetry breaking pattern has increased and the pattern is essentially made of two rows of spots. However, at some locations, the amplitude of the spot modulation decreases or even disappears (right end of Fig. 2(d), left end of Fig. 2(e)), giving place to a more or less uniform clear band. At the very end of the gel strip (right end of Fig. 2(e)), the two rows can fuse back into one. Indeed, the parts holding up the gel at each end may introduce defects of feed in the first and last

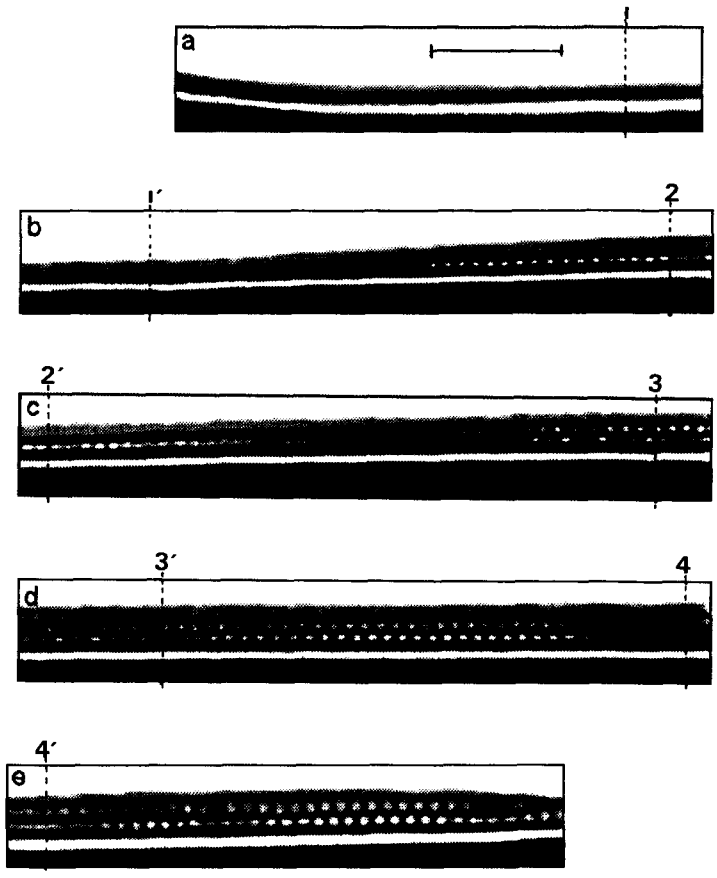

Fig. 2. Patterns in the bevelled thin strip. (a)–(e) are the binarized images of five successive portions of the strip. The whole pattern sequence can be reconstructed by placing side by side the five successive images. Pairs of vertical dotted lines (1 and 1′, 2 and 2′, etc.) indicate the same location along the strip. The bar inside (a) corresponds to 1 mm. (a) no symmetry breading pattern; (b) no symmetry breaking pattern and symmetry breaking pattern forming one row of spots; (c) transition region between one and two rows; (d) and (e) symmetry breaking pattern forming two rows of spots. Experimental conditions: concentrations of reagents in reservoir I: $[NaClO_2] = 0.0475\,M$, $[NaOH] = 1.2 \times 10^{-2}\,M$, $[KIO_3] = 2 \times 10^{-3}\,M$; in reservoir II: $[AM] = 1.3 \times 10^{-2}\,M$, $[H_2SO_4] = 10^{-2}\,M$; $[KI] = 2 \times 10^{-3}\,M$, $[Na_2SO_4] = 3 \times 10^{-3}\,M$; temperature = 4°C; residence time of reservoirs = 6 min.

5% along the length of the strip (see also the left end of Fig. 2(a)).

- The transition between one and two rows can be seen in Fig. 2(c). A magnification of such a transition region is given in Fig. 4. At the approach of the transition region, the modulation of the light intensity in the single row rapidly decreases: spots almost disappear. Then, as this fuzzy region becomes wider, a new clear spot pattern gains consistency. These spots elongate before separating in two spots of unequal sizes. The resulting pairs of spots first arrange obliquely in the pattern band. Then, as spots in the pairs become more equal in size and intensity, the pairs tilt in the direction of the feed gradient, giving rise to the appearance of a second row of spots. Progressively, a shift appears which then increases between the two spots of each pair. The final arrangement in two rows of perfectly staggered spots is reached at the right end of Fig. 4(b) (and in the middle part of Fig. 2(c)).

Thus, the emergence of the second row of spots as the width of the pattern region increases, is very progressive. It proceeds through some sort of spot division followed by the separation of the second

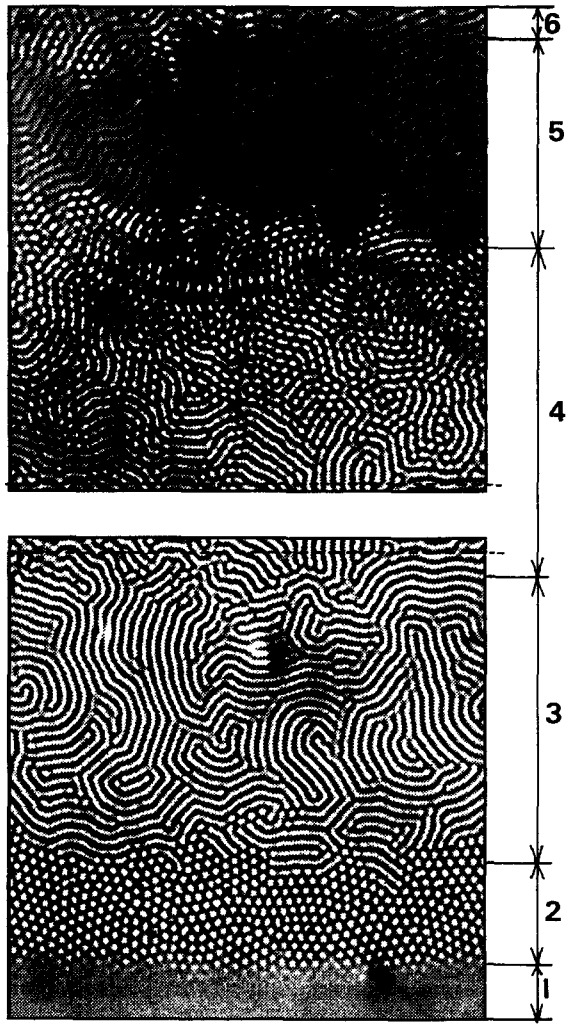

Fig. 3. Sequence of pattern in the bevelled disc. The whole sequence can be reconstructed by juxtaposing (a) and (b) and superposing the dotted lines at the top of (a) and at the bottom of (b). The various patterns extend over parallel bands. The vertical arrows delimit their successive domains: 1. uniform state (truncated at the bottom of the figure); 2. hexagonal array of spots; 3. stripes; 4. mixture of stripes and spots; 5. asymmetric stripes; 6. "non-standard" planforms. Experimental conditions as in Fig. 2(a) and (b): view size 6.9 mm × 6.9 mm.

row from the first one and by a progressive increase of the phase shift between spots in the two rows.

3.1.2. *In bevelled disc*

Each picture in Fig. 3 gives a view of about half the height of the disc in the median region; the lateral parts not shown bear the same types of patterns. The

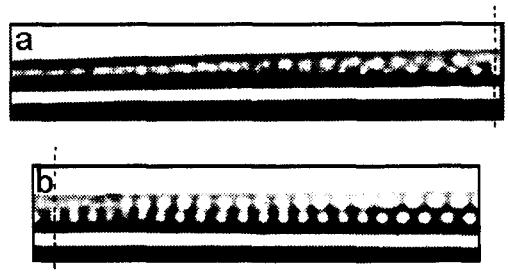

Fig. 4. The transition region between domains with one and two rows of spots, in the bevelled strip. The whole sequence can be reconstructed by placing side by side images (a) and (b). The vertical dotted lines indicate the same location along the strip. Form left to right in each figure: (a) fuzzy pattern with a few clear spots, spots of large size, spots splitting in two spots obliquely arranged; (b) pairs of spots arranged more or less perpendicularly to the feed boundary, two rows of staggered spots.

thickness of the disc progressively increases from the bottom of Fig. 3(b) to the top of Fig. 3(a). Patterns of different types extend over successive regions (numbered on the figure). These regions are almost parallel and organize as follows with the increasing thickness of the disc:

1 – a narrow uniform (structureless) region;
2 – a region of clear spots exhibiting a hexagonal arrangement;
3 – a wide domain of stripes;
4 – a region of complex organization exhibiting an intricate mixture of spots and stripes;
5 – a region of less contrasted, asymmetric stripes;
6 – a region of very intricate planform, located at the top of the disc.

The global organization can hold for days without significant modification of the general pattern. The area covered with patterns as well as the relative extent of the domain of each type of planform depend on the feed concentrations. The pictures of Fig. 3 were obtained with a chlorite concentration ($[NaClO_2]$) of 0.0475 M in the reservoir. In this case, the structureless region 1 extended over one eighth of the height of the disc. When $[NaClO_2]$ was increased by 30%, the extent of region 1 increased by a factor of 6. Conversely, a decrease of 5% of $[NaClO_2]$ resulted in the total disappearence of the uniform region; then the whole disc surgace was covered with patterns.

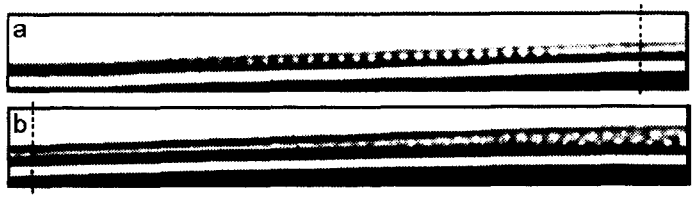

Fig. 5. Transient situation in the bevelled thin strip. The whole sequence can be reconstructed by placing side by side images (a) and (b). The vertical dotted lines indicate the same location along the strip. Note that the symmetry breaking pattern has disappeared over large lumps of the reactor. Picture taken 2 h after a 10% increase in the chlorite concentration. All other experimental conditions as in Fig. 2.

3.2. Transient situation

Asymptotic states as those presented above, in Figs. 2 and 3, are reached after about 10 h. Before this time, some remarkable transient situations can be observed, either when a new experiment is started or after a jump in the value of some chemical constraint during a series of experiments. In the latter case, the initial symmetry breaking patterns are erased over more or less extended parts of the gel reactors. In Sections 3.2.1 and 3.2.2, we shall examine transient situations observed after a 10% increase in the chlorite concentration.

3.2.1. In bevelled thin strip

Fig. 5 shows a transient situation in the bevelled gel strip. The symmetry breaking pattern was completely erased (see right end of Fig. 5(a) and left end of Fig. 5(b)) over a large extent comprised between the region with one row of spots (Fig. 5(a)) and the transition region (right end of Fig. 5(b)). At both ends of this now uniform clear band, patterns are similar to those observed in the initial asymptotic state. After this transient situation, the system evolves towards a new asymptotic state: spots slowly reinvade this temporally featureless band while, at the other end of the row, spots disappear and the region without symmetry breaking pattern gains in extension in the narrowest parts of the bevelled strip.

3.2.2. In bevelled disc

An equivalent transient situation is observed in the bevelled disc reactor, Fig. 6. The patterns in regions 3 and 4 are transiently erased. Then during the evolution towards the new steady state, stripes progressively reinvade this temporary uniform region. However, the expanding stripe region is preceded by a region tesselated with hexagonal arrays of dark spots. This remarkable new hexagonal patterns could never be stabilized in any of the tested asymptotic states. Note that these patterns are relatively long-lived since they have been observed for about 8 h. Ultimately, the stripe structure spreads over the whole area, and a pattern sequence similar to that of Fig. 3 is recovered.

4. Discussion

It is worth noting that, in the thin strip reactor, essentially one type of symmetry breaking pattern is observed, i.e. spots arranged in rows parallel to the feed boundaries. However, in the transition region between one and two rows, there can be different stationary phase relations between the peaks in two rows. As already mentioned, in a very thin strip ($h \leq \lambda$), one row of spots can be thought as the experimental approximation of a one-dimensional Turing pattern. In a genuine uniformly constrained (theoretical) one-dimensional reaction – diffusion system, the only possible stationary symmetry breaking pattern is a periodic longitudinal amplitude modulation. In an ideally thin two-dimensional system with a strong parameter gradient in one direction, theoretical simulations show that the Turing pattern emerges as a single row of spots perpendicular to the gradient. This pattern is shown to have the same bifurcation properties as a one-dimensional system [9]. Our experiments are usually performed in gel strips with a thickness comparable to the wavelength of the pattern ($h \cong \lambda$). The observed

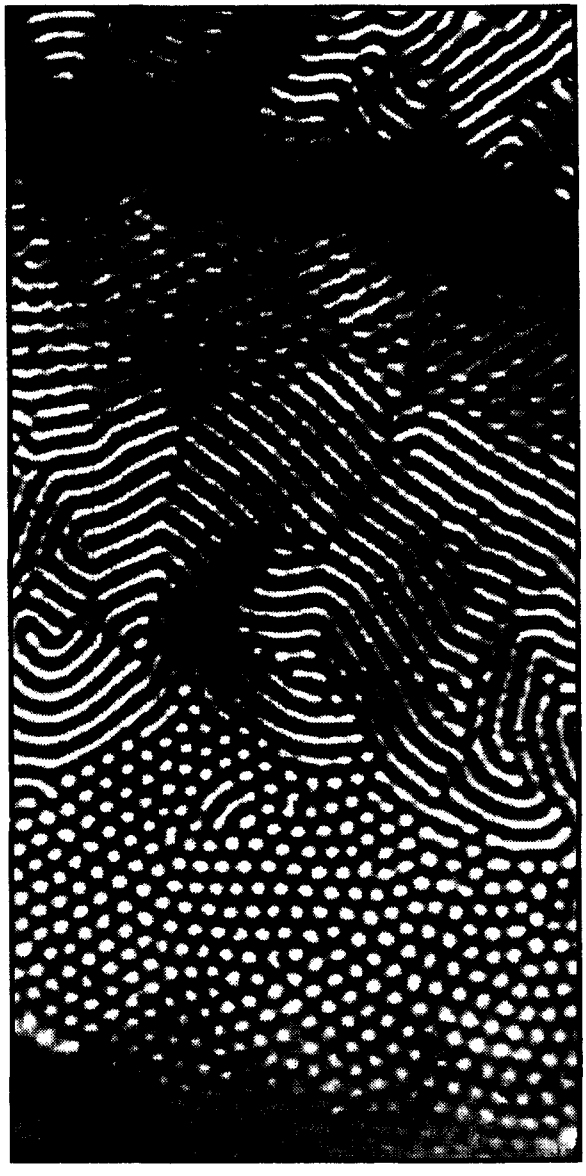

Fig. 6. Transient pattern sequence in the bevelled disc. Note that, as in Fig. 5, the pattern has disappeared over large extents; see the region of homogeneous state located in the upper parts of the figure; see also the black hexagons at the borders of this region. Picture taken 2 h after 10% increase in the chlorite concentration. All other experimental conditions as in Fig. 3.

"quasi-one-dimensional" pattern can actually be made either of short columns perpendicular to the observation plane or of beads, and no distinction can be made between a column and a bead pattern. However, as we have mentioned, in the widest parts of the bevelled gel strip, at some places, spots inside one row become fuzzy or even disappear, giving place to segments of clear bands. Such segments can be understood as columns layed parallel to the impermeable boundaries. Another possibility is that, due to a difficult rearrangement of a number of spots emerging in a limited space inside the row, the corresponding zone in the pattern region exhibits a vanishing amplitude modulation. Such segments can be considered as defects of the pattern. The capability of the system to eliminate such defects seems very limited since these clear segments held unchanged for about two days, the usual duration of an experiment.

The diversity of patterns observed in the bevelled disc reactor will be better understood when comparing these observations with those made in the bevelled strip reactor at locations with comparable distances between the feed boundaries. We thus compare in the two reactors, locations with the same width of pattern-forming region. However, if the gel strip reactor provides information on the number of separated pattern layers, in any case it can provide information on the type of pattern selected in the layers that develop in the disc reactor.

In the thinnest region of the disc as in the narrowest part of the strip, no symmetry breaking pattern develops. The region of the gel strip where pattern is made of one row of spots fits regions 2 and 3 in the disc over which hexagonal arrays of clear spots and stripe patterns can be seen. Thus, these patterns correspond to genuine monolayer patterns. In these monolayers, the spot and stripe patterns actually correspond, respectively, to bead and column structures. Note that these columns are seldom straight but generally bent columns. In the following, they will be simply referred as "columns". The spot and stripe patterns in regions 2 and 3 of the disc are characterized by their relative sharpness. Such hexagon and stripe patterns have initially been observed by Ouyang and Swinney [17,18] and later by others [23] and thought as effective quasi-two-dimensional patterns. It has been shown theoretically that, at onset, monolayers of Turing patterns have the same qualitative bifurcation diagram and pattern selection properties than two-dimensional systems [7,9]. The hexagonal mode is generally the

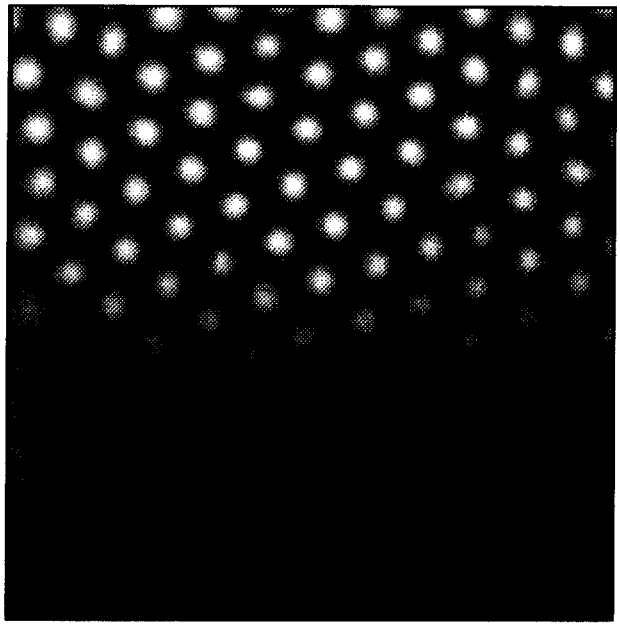

Fig. 7. The transition between the domains of uniform state and hexagon pattern. Magnification of a small region.

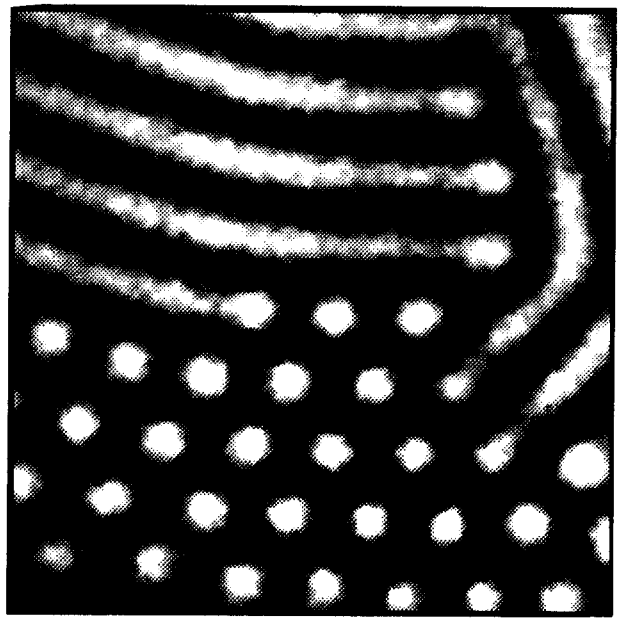

Fig. 8. The transition between the domains of hexagon and stripe patterns. Magnification of a small region.

first stable mode and appears subcritically; the stripe mode becomes stable only at some distance from onset while hexagons loose their stability. The stability domains of these two modes overlap over some range of bifurcation parameter values. However, there is an important difference between genuine two-dimensional systems and monolayers: in the latter, the hexagonal mode is generically restabilized at some distance from onset [7,9]. Note that the sequence uniform–hexagons–stripes experimentally observed in the bevelled disc, follows exactly the stability order predicted by the linear stability analysis. In the asymptotic state we usually observe a very sharp transition between the uniform state and the hexagon pattern, i.e. the amplitude suddenly damps within a wavelength (see Fig. 7) which is consistent with the subcritical nature of the bifurcation to hexagons. However, we have never observed any obvious hysteresis in the position of this transition front as a function of feed parameters. Such hysteresis could be expected as a result of a front pinning due to non-variational effects. The same sharp transition is observed between hexagon (region 2) and stripe (region 3) patterns (see Fig. 8). No mixed state is observed at this front. This is consistent with the discontinuous nature of the transition between the stable hexagonal and striped modes. Here again no noticeable hysteresis is found as a function of constraints, contrary to another report [21]. No pinning is observed in our experimental conditions which infers a weak overlap of the stability domains of hexagons and stripes.

The intricate pattern in region 4 is made of modulated stripes and it is very tempting to think of this pattern as a mixed mode. However, in the classical two-dimensional approach, this mixed mode is unstable [31]. The modulated stripes of region 4 develop in the continuation of the regular stripes of region 3. Modulations are regularly spaced along the stripes and form a hexagonal array of higher light intensity. Region 4 in the bevelled disc of gel would correspond to the transition region where a second row of spots is seen to progressively emerge in the bevelled strip. This occurs when the width Δ of the pattern-forming region exceeds a critical size. Region 4 in the disc can be understood as a region where a second layer of pattern is building up; a truely three-dimensional pattern is unfolding here. Fig. 9 provides a magnification of the transition region between regions 3 and 4: At the frontier with region 3, spots are few and have

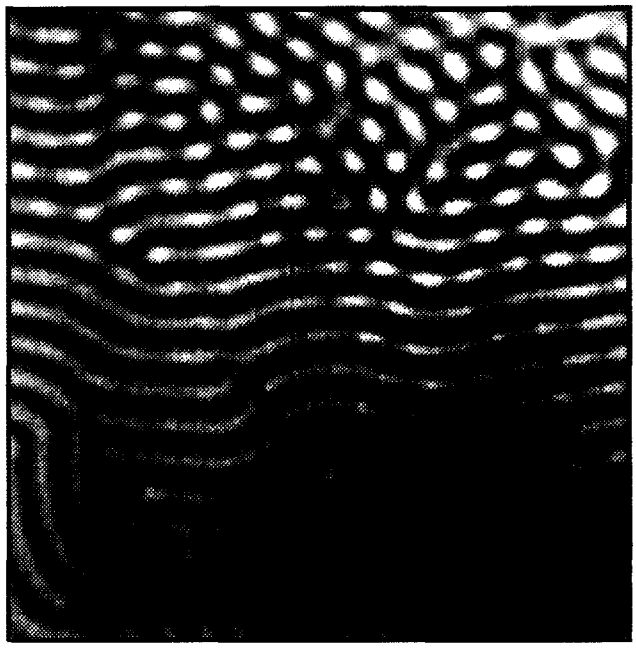

Fig. 9. Detailed view of the transition zone between regions 3 and 4. Note the hexagon–stripe mixed pattern.

a low amplitude. Going upwards, towards region 5, spots along the stripes become more numerous and regularly spaced. In the light of our observations in the gel strip, we conjecture that these spots develop as outgrowths on the columnar structure of the first pattern layer. Note that the spots stay basically centred along the clear columns.

Subsequently, with the increased thickness of the disc of gel, outgrowths would form an extra roll along the initial columns, so that we can understand the structure in region 5 as being formed of two layers of parallel columns. Region 5 in the disc corresponds in the gel strip to the regions with two rows of spots either with a slight shift between splitting pairs or completely staggered spots. Generally, in region 5, the columns of the second layer do not settle at equal distance from two neighbour columns in the first layer but rather stay closer to one of them. The projection of such a three-dimensional arrangement on the plane of the picture results in a pattern made of stripes with poorer constrast than in region 3. A magnification of such a picture with enhanced constrast is given in Fig. 10 with the light intensity profile taken along a line perpendicular to the direction of the stripes. The profile shows a period made of two peaks with two unequal heights. This can be understood as the superposition of two non-harmonic modulations of the light intensity. Note that non-harmonic modulations are generally expected far from onset. The non-symmetric shape of the profile could result either from a phase shift actually slightly less than half a wavelength between the columns in the two layers (as suggested also by the observations in the bevelled strip reactor) or from a bias in the observation direction of a symmetric array of staggered columns. Our observations in the strip reactor seem to favour the first assumption.

Thus, we have observed the emergence of a second layer of pattern which, in region 4, is made of a hexagonal array of beads more or less separated from the columns of the first pattern layer; these beads transform into parallel columns in region 5 and the sequence hexagon–stripe experimentally observed for the first layer repeats in the second one. This means that various layers of patterns can develop at different distances from the feed boundaries, and each layer can undergo, somewhat independently, the same pattern

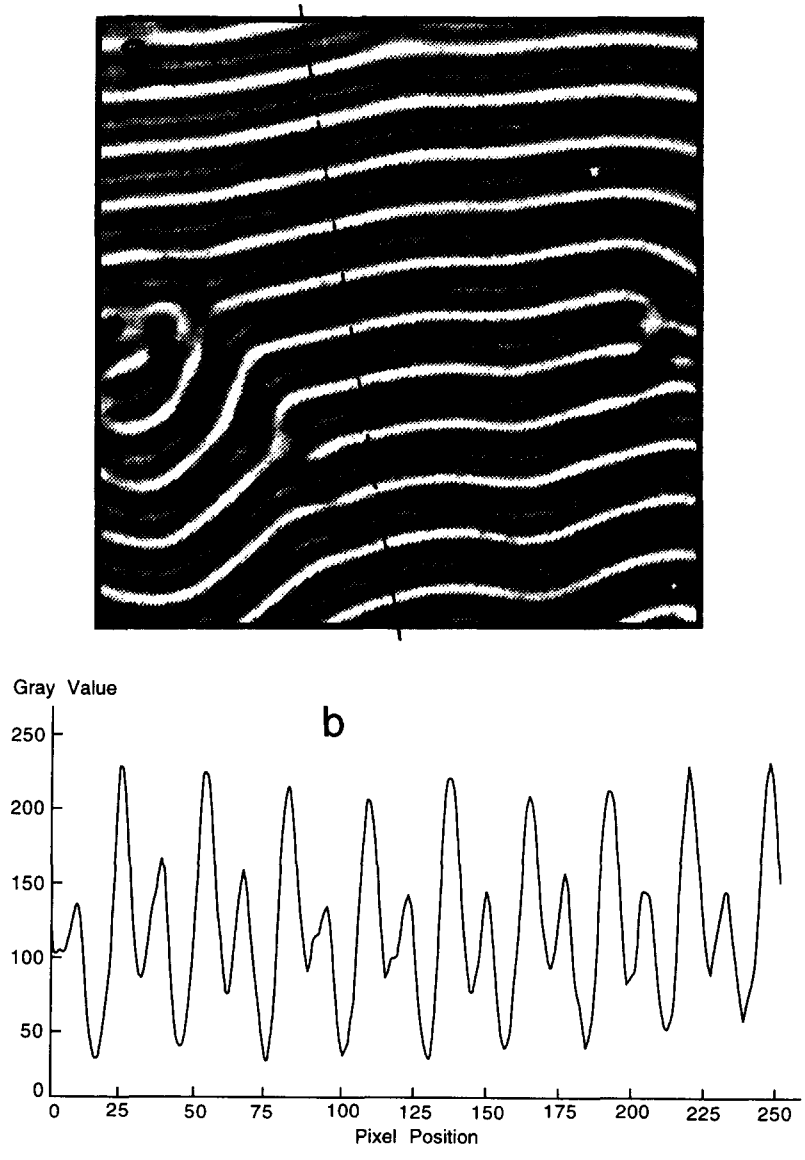

Fig. 10. The asymmetric stripes of region 5: (a) a magnification; (b) the light intensity profile along the line (-------) drawn in picture (a).

mode sequence as the thickness of the disc reactor increases. Moreover, different planforms can be observed at a given disc thickness, in adjacent layers. This is in agreement with preliminary theoretical [24] as well as experimental [21] results obtained in three-dimensional systems in the presence of parameter gradients.

At first glance, region 6 exhibits a wealth of very intricate planforms. However, a closer examination of these apparently different planforms brings the conclusion that they are various aspects of the same basic organization. Such patterns typically appear as illustrated in Fig. 11. Planforms of this type are observed at the top of the disc, as in Fig. 3. Such regions of the bevelled disc correspond to regions of the bevelled strip where the pattern is made of two rows of spots; so that the planform of Fig. 11 can be considered as the projection on the observation plane of two patterns

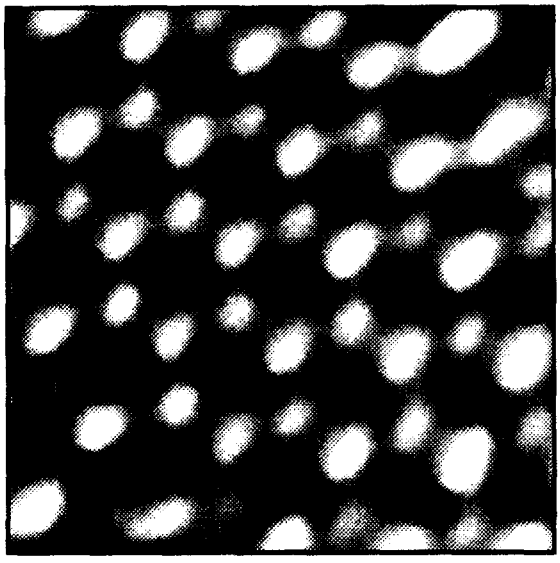

Fig. 11. An example of intricate planform commonly observed in region 6.

that develop in two adjacent layers. Such non-standard planforms are rather difficult to elucidate. They can be understood as moiré images of standard planforms. Patterns very similar to those of region 6 can be obtained by summing an image of hexagonal array of clear spots and an image of stripes from regions 2 and 3, with the clear spots superposed to the dark stripes. Note the necessary phase shift of π compared to the superposition that produces planforms such as those observed in region 4. This superposition of spots and stripes in region 6 implies that a spot pattern is restabilized in the top of the disc reactor, Such a restabilization of the hexagonal mode is also found in many computations and analytical calculations on the Brusselator [7,32] and the Schnackenberg [8,9] models. This phenomen is often referred as reentrance.

Another case of reentrance is obtained in the transient shown in Fig. 6 which exhibits the sequence uniform – clear hexagons – stripes – dark hexagons – uniform. This can be thought as two different Turing bifurcations from uniform to hexagons, one of them from uniform to clear hexagons, and the other from uniform to dark hexagons. This can be theoretically understood if the quadratic term of the normal form of the Turing bifurcation changes sign. Note that dark hexagons have always been observed as transient in experiments. It is also remarkable that dark spots were never observed in the bevelled strip, even transiently.

Let us now consider again the uniform state next to the dark hexagons. This region has to be associated to the temporary featureless clear band in the strip reactor (Fig. 5). In the disc reactor, this should then correspond to a clear sheet which could constitute the first element of a lamellar structure predicted by theory in three-dimensional systems [10]. As the black hexagons, this structure is unstable under our experimental conditions.

5. Conclusion

We have used an indirect approach in order to address the problem of the actual pattern organization in three-dimensional systems, in the presence of feed gradients. Indeed, there is a severe technical obstacle to the direct analysis of three-dimensional structures: the structures correspond to smooth continuous changes in concentration of diluted species and the contrast of patterns decreases with the decrease of the focal depth. The direct analysis would call for focal depth much smaller than the wavelength of the pattern, that is of the order of a few hundredth of millimeter; in these conditions, contrast would be so low that very low noise camera and frame average techniques should be used much in the same way as in confocal microscopy. Other authors seem to have made a rough measurement of the thickness and position of the pattern-forming region [33]. However, as mentioned by these authors, the accuracy of their method heavily depends on the pattern contrast which can decrease from one layer to the next, making difficult the actual determination of the number of layers.

Our innovative approach consisted in designing reactors that enable to slowly unfold the pattern transitions along one direction of the reactors. These reactors can be thought of as the non-linear chemistry analogues of the Kofler hot stage used in the determination of equilibrium phase transitions. In our reactors, the uniform–hexagon–stripe transition sequence classically predicted in theoretical studies, was directly viewed, unfolded in space. The continous

follow up of pattern evolution allowed us to draw some conclusions on bilayer patterns. In particular, we have been able to follow the emergence of a bilayer from a monolayer pattern and have shown that this transition is progressive.

The presence of steep feed gradients seems to make the three-dimensional pattern selection mechanism resourceful through the coupling of basic patterns. In our experiments these are the basic two-dimensional hexagonal and stripe modes. The main question which is still to be solved is that of the determination of the possible stable phase relations that can exist between the patterns in the two layers. Our observations suggest that several such phase shifts are possible and that the relative stability of these phase relations may depend on the constraints and probably on the exact shape of the confining parameter well. However, the method becomes unreliable for more than two patterned planes.

Note that in this series of experiments, we have not identified patterns that could result from the superposition of two layers of hexagons. However, triangular patterns observed in other experiments [34] suggest that the superposition of a clear and a dark hexagon layers is possible. Refined experiments with our bevelled reactors are now in progress. Moreover in new sets of experiments, the spatio-temporal behaviours [23] that result from the superposition of a temporal instability (Hopf) in one plane and a spatial instability (Turing) in another are distinguished from behaviours that develop in a single stratum of width Δ comparable to the Turing wavelength λ. This will be the subject of a forthcoming paper.

Acknowledgements

The authors are indebted to Dr. Jacques Boissonade for stimulating discussions and for sharing the results of his numerical simulations prior to publication.

References

[1] V. Castets, E. Dulos, J. Boissonade and P. De Kepper, Phys. Rev. Lett. 64 (1990) 2953.
[2] A.M. Turing, Philos. Trans. Roy. Soc. London B 327 (1952) 37.
[3] G. Nicolis and I. Prigogine, Self Organization in Nonequilibrium Chemical Systems (Wiley, New York, 1977).
[4] J.D. Murray, Mathematical Biology (Springer, Berlin, 1989).
[5] H. Meinhardt, Models of Biological Pattern Formation (Academic Press, New York, 1982).
[6] L.G. Harrison, Int. J. Plant Sci. 153 (1992) S76.
[7] P. Borckmans, A. De Wit and G. Dewel, Physica A 188 (1992) 137.
[8] V. Dufiet and J. Boissonade, J. Chem. Phys. 96 (1992) 664.
[9] V. Dufiet and J. Boissonade, Physica A 188 (1992) 158.
[10] A. De Wit, G. Dewel, P. Borckmans and D. Walgraef, Physica D 61 (1992) 289.
[11] M. Herschkowitz-Kaufman and G. Nicolis, J. Chem. Phys. 56 (1972) 1980; J.F. Auchmuty and G. Nicolis, Bull. Math. Biol. 37 (1975) 323.
[12] T.C. Lacalli, D.A. Wilkinson and L.G. Harrison, Development 104 (1988) 105.
[13] A. Hunding and M. Brons, Physica D 44 (1990) 285.
[14] J. Boissonade, J. Physique (France) 49 (1988) 541.
[15] P. De Kepper, V. Castets, E. Dulos and J. Boissonade, Physica D 49 (1991) 161.
[16] J. Boissonade, V. Castets, E. Dulos and P. De Kepper, Int. Ser. Num. Math. 97 (1991) 67.
[17] Q. Ouyang and H.L. Swinney, Nature 352 (1991) 610.
[18] Q. Ouyang and H.L. Swinney, Chaos 1 (1991) 411.
[19] J.J. Perraud, K. Agladze, E. Dulos and P. De Kepper, Physica A 188 (1992) 1.
[20] R.D. Vigil, Q. Ouyang and H.L. Swinney, Physica A 188 (1992) 17.
[21] Q. Ouyang, Z. Noszticzius and H.L. Swinney, J. Chem. Phys. 96 (1992) 6773.
[22] K.L. Lee, Q. Ouyang, W.D. McCormick and H.L. Swinney, preprint.
[23] P. De Kepper, J.J. Perraud, B. Rudovics and E. Dulos, Int. J. Bif. Chaos 4 (1994) 1215.
[24] J. Boissonade, E. Dulos and P. De Kepper, in: Chemical Waves and Patterns, eds. R. Kapral and K. Schowalter (Kluwer Academic Publishers, Dordrecht, 1995) 221.
[25] Z. Noszticzius, Q. Ouyang, W.D. McCormick and H.L. Swinney, J. Chem. Phys. 96 (1992) 6302.
[26] P. De Kepper, I.R. Epstein, K. Kustin and M. Orbán, J. Phys. Chem. 86 (1982) 170.
[27] I. Lengyel and I.R. Epstein, Science 251 (1990) 650.
[28] I. Lengyel and I.R. Epstein, Proc. Nat. Acad. Sci. USA 89 (1992) 3977.
[29] J.E. Pearson and N.J. Bruno, Chaos 2 (1992) 513.
[30] K. Agladze, E. Dulos and P. De Kepper, J. Phys. Chem. 96 (1992) 2400.
[31] A. De Wit, G. Dewel and P. Borckmans, Phys. Rev. E 48 (1993) R4191.
[32] G. Dewel, P. Borckmans, A. De Wit, B. Rudovics, J.J. Perraud, E. Dulos, J. Boissonade and P. De Kepper, Physica A 213 (1995) 181.
[33] I. Lengyel, S. Kádár and I.R. Epstein, Phys. Rev. Lett. 69 (1992) 2729.
[34] B. Rudovics, Ph.D. Thesis, Bordeaux, France (1995).